JOURNAL OF VIROLOGY, Sept. 2011, p. 8646–8655 Vol. 85, No. 17
0022-538X/11/$12.00 doi:10.1128/JVI.02559-10

The Cellular RNA Helicase UAP56 Is Required for Prevention of Double-Stranded RNA Formation during Influenza A Virus Infection▽†

Christian Wisskirchen,[1,2] Thomas H. Ludersdorfer,[1,2] Dominik A. Müller,[1] Eva Moritz,[1] and Jovan Pavlovic[1]*

Institute of Medical Virology, University of Zurich, Winterthurerstrasse 190, 8057 Zurich, Switzerland,[1] and Ph.D. Program in Microbiology and Immunology, University of Zurich, Zurich, Switzerland[2]

Received 9 December 2010/Accepted 1 June 2011

The cellular DEAD box RNA helicase UAP56 plays a pivotal role in the efficient transcription/replication of influenza A virus. UAP56 is recruited by the nucleoprotein (NP) of influenza A viruses, and recent data revealed that the RNA helicase is required for the nuclear export of a subset of spliced and unspliced viral mRNAs. The fact that influenza viruses do not produce detectable amounts of double-stranded RNA (dsRNA) intermediates during transcription/replication suggests the involvement of cellular RNA helicases. Hence, we examined whether the RNA-unwinding activity of UAP56 or its paralog URH49 plays a role in preventing the accumulation of dsRNA during infection. First, our data showed that not only UAP56 but also its paralog URH49 can interact with NPs of avian and human influenza A viruses. The small interfering RNA (siRNA)-mediated depletion of either RNA helicase reduced the transport of M1 and hemagglutinin (HA) mRNAs and, to a lesser extent, NP and NS1 mRNAs into the cytoplasm. Moreover, we found that virus infection of UAP56-depleted cells leads to the rapid accumulation of dsRNA in the perinuclear region. In parallel, we observed a robust virus-mediated activation of dsRNA-dependent protein kinase R (PKR), indicating that the cellular RNA helicase UAP56 may be recruited by influenza virus to prevent dsRNA formation. The accumulation of dsRNA was blocked when actinomycin D or cycloheximide was used to inhibit viral transcription/replication or translation, respectively. In summary, we demonstrate that UAP56 is utilized by influenza A viruses to prevent the formation of dsRNA and, hence, the activation of the innate immune response.

Influenza A viruses cause a highly contagious respiratory disease in humans and have been responsible for periodic widespread epidemics, or pandemics, that have caused high mortality rates (22). The most devastating pandemic occurred in 1918, resulting in 20 to 50 million deaths worldwide. Influenza viruses are enveloped, and their genomes consist of eight negative-stranded RNA segments coding for at least 10 proteins. While the majority of their viral mRNAs are intronless (mRNAs of segments 1 to 6), segments 7 (M) and 8 (NS) generate spliced as well as unspliced mRNAs (16). The viral genome is transcribed and replicated within the host cell nucleus by the virus-encoded RNA-dependent RNA polymerase complex consisting of the three subunits PB1 (protein basic 1), PB2, and PA (protein acidic) in the cell nucleus. The synthesis of viral mRNA involves a "cap-snatching" mechanism, whereby the cap structures of cellular precursor mRNA are cleaved 12 to 15 nucleotides downstream of the cap by the endonuclease activity of PA (6). The capped oligonucleotides serve as primers for the initiation of the viral mRNA synthesis. The replication of viral genomic RNA involves the synthesis of a positive-stranded complementary intermediate (cRNA) of the genomic RNA. Since the genome of influenza viruses does not encode a helicase, which is required for the unwinding of double-stranded RNA (dsRNA) replicative intermediates, it has been suggested that the influenza virus polymerase complex may recruit cellular RNA helicases. In support of this, Momose and colleagues demonstrated previously that the nucleoprotein (NP) of influenza A virus binds to the DEAD box helicase UAP56 and that this interaction leads to increased viral RNA (vRNA) synthesis *in vitro* (21).

UAP56 plays a pivotal role in spliceosome assembly as well as the export of spliced and unspliced mRNAs from the nucleus into the cytoplasm. UAP56 was first identified as an essential splicing factor that is required for prespliceosome and mature spliceosome assembly (9, 33, 34). In addition, UAP56 plays an important role in the nuclear export of mRNA into the cytoplasm (18). Hereby, UAP56, as part of the transcription export complex (TREX), recruits the Aly/REF nuclear export adaptor protein to the exon-junction complex (EJC) bound to pre-mRNAs and delivers it to the export receptor NXF1 (4, 31). Furthermore, UAP56 appears to be involved in the proper translocation of mRNAs in the cytoplasm (20).

URH49/DDX39 is a paralog of UAP56, exhibiting 90% amino acid identity. URH49 appears to have a function very similar to that of UAP56 in nuclear RNA export (15, 27). Like UAP56, URH49 is able to interact with the nuclear export adaptor protein Aly and can partially complement the function of Sub2p, the yeast homolog of UAP56 (27). Both URH49 and UAP56 can be detected in all mammalian cells and tissues but

* Corresponding author. Mailing address: Institute of Medical Virology, University of Zurich, Winterthurerstrasse 190, 8057 Zurich, Switzerland. Phone: 41 44 634 2656. Fax: 41 44 634 4906. E-mail: pavlovic.jovan@virology.uzh.ch.

† Supplemental material for this article may be found at http://jvi.asm.org/.

▽ Published ahead of print on 15 June 2011.

exhibit different expression profiles. While the URH49 expression level is clearly increased in proliferating cells, UAP56 levels remain constant (27). The concomitant downregulation of URH49- and UAP56-specific small interfering RNAs (siRNAs) leads to the retention of poly(A)$^+$ RNA in the nucleus and to cell death within 72 h (15). So far, there are no data available that would link URH49 to spliceosome assembly or the cytoplasmic targeting of mRNPs.

Growing evidence suggests that influenza viruses exploit the primary cellular mRNA nuclear export pathway for directing their mRNAs to the cytoplasm (2, 28, 38). Subsets of spliced and unspliced influenza virus mRNAs are exported into the cytoplasm in a UAP56/NFX1-dependent fashion. Read and Digard (28) recently showed that UAP56 is involved in the nuclear export of M1, M2, and NS1 mRNAs, while the export of other viral mRNAs, such as those encoding NS2, NP, and hemagglutinin (HA), appear to be independent of UAP56. Hence, UAP56 participates in the nuclear export of spliced as well as unspliced viral mRNAs. In contrast, the nuclear export of genomic viral RNPs (vRNPs) is mediated by the CRM-1 pathway independent of UAP56 (8).

In this study we first sought to determine whether UAP56 and URH49 play a role in the replication/transcription of influenza virus RNA. We observed that both URH49 and UAP56 interact with the NP protein from both avian and human influenza virus strains. Using siRNAs specific for either URH49 or UAP56, we found that the downregulation of UAP56 or URH49 reduced the accumulation of NP mRNAs in the cytoplasm. Most interestingly, we found that virus infection of cells with downregulated UAP56 leads to the rapid accumulation of dsRNA in the perinuclear region. In parallel, we observed a robust virus-dependent activation of dsRNA-dependent protein kinase R (PKR) in these cells, indicating that the function of the cellular UAP56 RNA helicase may be redirected by the influenza virus to evade the antiviral function of the type I interferon (IFN) system.

MATERIALS AND METHODS

Cells and viruses. A549 and HEK 293T (ATCC) cells were cultured in Dulbecco's modified Eagle's medium (DMEM) (Gibco) supplemented with 10% fetal calf serum (FCS), 1% penicillin-streptomycin (Gibco), and 1% Glutamax (Gibco). The human influenza virus strain A/PR8/34/H1N1 (PR8), the avian influenza virus strain A/Bratislawa/79/H7N7 (fowl plague virus [FPV]), and vesicular stomatitis virus (VSV) Indiana were previously described (26). Infections were carried out with DMEM, 2% FCS, 1% penicillin-streptomycin, and 1% Glutamax for FPV and VSV. For PR8, DMEM with 0.2% bovine serum albumin (BSA) (Roth), 1% penicillin-streptomycin, 1% Glutamax, and 0.5 μg/ml trypsin was used. Cells were washed once with infectious medium; afterwards, infections were done for 30 min at room temperature, virus was aspirated, and the cells were incubated in infectious medium for the indicated amounts of time. Viral titers were determined as the 50% tissue culture infective dose ($TCID_{50}$) with supernatants from infected cells. Madin-Darby canine kidney (MDCK) cells were used for virus titrations. Titrations were performed, as previously described (26), at least four times for each virus. Statistical significance was determined by using the paired *t* test.

Transfections and siRNA knockdowns. 293T cells were transfected at 80% confluence with jetPEI transfection reagent (Polyplus transfection) according to the instructions of the manual. Validated stealth siRNAs were purchased from Invitrogen, and medium GC control siRNA (12935-300; Invitrogen) and validated pooled siRNAs were used against URH49 (DDX39HSS141113, DDX39HSS141114, and DDX39HSS141115; GenBank accession number NM_005804.2) and UAP56 (BAT1HSS111847, BAT1HSS111848, and BAT1HSS111849; accession number NM_004640.5). siRNA transfections were done by using HiPerFect (Qiagen) according to the manufacturer's instructions. Transfections were performed in suspension using 6×10^4 cells per 24-well and 30 nM siRNA. Knockdowns were confirmed via Western blot analysis and quantitative PCR (qPCR).

Western blot and coimmunoprecipitation assays. 293T cells were grown in 10-cm cell culture dishes (Techno Plastic Products [TPP]) and transfected at 80% confluence with the indicated amounts of plasmid. Forty-eight hours after transfection cells were lysed in 500 μl lysis buffer (0.5% Triton X-100, 20 mM Tris [pH 7.5], 100 mM NaCl, 50 mM β-glycerolphosphate, 50 mM sodium fluoride, 1 mM sodium orthovanadate, and a protease inhibitor cocktail [Roche]). Coimmunoprecipitations were performed with 1 μg mouse anti-FLAG antibodies (Sigma) for 4 h at 4°C. Immunoprecipitations were done at room temperature for 1 h by using 50 μl of protein G beads (Dynalbeads; Invitrogen). Samples were washed three times with lysis buffer, and beads were taken up in 40 μl SDS-Laemmli buffer and heated for 5 min to 95°C. Samples were loaded onto 10% SDS gels, followed by immunoblot analysis with different antibodies. Anti-FLAG antibody (1:3,000; Sigma) against mouse and rabbit, anti-URH49 (1:750; Acris), anti-UAP56 antibody (serum from a mouse immunized with a peptide of human UAP56), anti-NP mouse monoclonal antibody HB65 (1:3), and polyclonal serum against influenza A virus (FLUAV) (1:1,500) and anti-actin (1:2,000; Santa Cruz Biotechnologies [SCBT]) were used. Anti-PKR and -phospho-PKR (1:2,000; Abcam) and anti-FLUAV M1 HB64 (1:3; ATCC) antibodies were also used. Primary antibodies were incubated overnight at 4°C and incubated the next day for 1 h with anti-horseradish peroxidase (HRP)-conjugated secondary antibodies from GE-Healthcare (1:10,000). Membranes were analyzed with a Fuji imager using Multi Gauge 3.0 software.

Indirect immunofluorescence analysis. A549 cells were transfected with siRNA as indicated and grown on chamber slides for 72 h. Cells were infected at a multiplicity of infection (MOI) of 5 with FPV or PR8, fixed at the indicated times postinfection (p.i.) with 4% paraformaldehyde, and permeabilized with 0.5% Triton X-100 in phosphate-buffered saline (PBS). Cells were washed twice with PBS and blocked for 30 min with 1% BSA. Primary and secondary antibodies were diluted in 1% BSA and incubated for 1 h at room temperature in the dark. Cells were washed three times after each step. Anti-dsRNA J2 antibody (1:4,000; Engscicons, Hungary) and rabbit anti-FLUAV serum (1:300) were used as primary antibodies. As secondary antibodies, Alexa 488 anti-rabbit and Alexa 594 anti-mouse (1:1,000; Invitrogen) antibodies were used. Cycloheximide (75 μg/ml) and actinomycin D (0.5 μg/ml) were diluted from 10-mg/ml stocks in normal DMEM and incubated with the cells from 1 h before infection until fixation of the cells. Slides were mounted in Fluoromount mounting medium containing 4′,6-diamidino-2-phenylindole (DAPI) (Southern Biotech). Samples were analyzed with a Leica TCS SP5 microscope using LAF software.

Expression constructs and protein purification. URH49 and UAP56 were cloned into pGEX-3x (GE Healthcare) with an N-terminal glutathione (GSH) *S*-transferase (GST) fusion tag (URH49-for [5′-GATAAGAATTCCGCAGAACAGGATGTGGAAAACGATC-3′ {EcoRI}], URH-49-rev [5′-CTAATGAATTCAATTTACCGGCTCTGCTCGATGTATGTG-3′ {EcoRI}], UAP56-for [5′-CTTATACCCGGGGCAGAGAACGATGTGGACAATG-3′ {SmaI}], and UAP56-rev [5′-CAATAATCCCGGGATAAACTACCGTGTCTGTTCAATGTA-3′ {SmaI}]).

Proteins were expressed in *Escherichia coli* BL21 cells with 0.1 mM isopropyl-β-D-thiogalactopyranoside (IPTG) for 4 h at 32°C. Bacteria were harvested and lysed by 6 cycles of sonication for 30 s in Tris lysis buffer (50 mM Tris-HCl [pH 8.0], 500 mM NaCl, 0.1% NP-40, 5 mM $MgCl_2$, 10 mM 2-mercaptoethanol, 10% glycerol, protease inhibitor cocktail [Roche]). Lysates were cleared at 12,000 × *g* for 20 min and applied onto a glutathione-Sepharose column (Glutathione Sepharose High Performance; GE Healthcare). Bound proteins were washed with Tris wash buffer (50 mM Tris-HCl [pH 8.0], 100 mM KCl, 0.1% NP-40, 5 mM $MgCl_2$, 10 mM 2-mercaptoethanol, 10% glycerol), eluted with Tris elution buffer (20 mM Tris-HCl [pH 8.0], 100 mM KCl, 0.1% NP-40, 5 mM $MgCl_2$, 5 mM 2-mercaptoethanol, 10 mM reduced glutathione, 20% glycerol), and dialyzed against elution buffer without GSH. PR8-NP and FPV-NP were cloned into pQE-32 vectors (Invitrogen) containing an N-terminal 6×His tag by using the following primers: PR8-NP-for (5′-GATTATCCCGGGGCGTCTCAAGGCACCAAACGATC-3′ [SmaI]), PR8-NP-rev (5′-CATTAGGTCGACTTATCGTATTCCTCTGCATTGTC-3′ [SalI]), FPV-NP-for (5′-CATTACCCGGGGCGTCTCAAGGCACCAAACGATCTTATG-3′ [SmaI]), and FPV-NP-rev (5′-CGTAATCCCGGGGATTAATTAATTGTCATACTCCTCTGCATTGTCTC-3′ [SmaI]). Proteins were expressed in *E. coli* M15 pRep4 cells with 1.5 mM IPTG overnight at 22°C. Bacteria were harvested and sonicated 6 times for 30 s in Tris lysis buffer containing 50 mM imidazole. The resulting lysates were cleared at 12,000 × *g* for 20 min, applied onto Ni-nitrilotriacetic acid (NTA) columns (Qiagen), washed with Tris wash buffer containing 50 mM imidazole, eluted with elution buffer (as

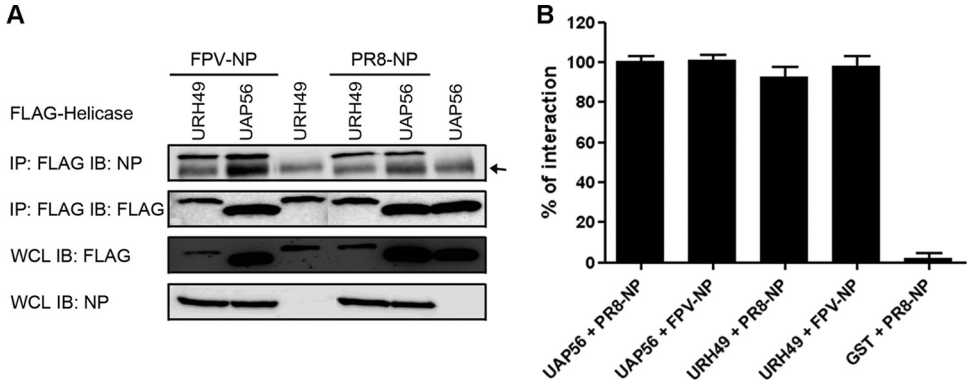

FIG. 1. Human and avian influenza A virus nucleoproteins interact with the cellular helicases UAP56 and URH49. (A) Coimmunoprecipitation assays were performed with FLAG-tagged UAP56 or URH49 and avian or human influenza A virus nucleoproteins. The arrow indicates the position of the heavy chain of the antibodies used for immunoprecipitation (IP). IB, immunoblot; WCL, whole-cell lysate. (B) Affinity-purified GST-UAP56 or GST-URH49 and His-PR8-NP (A/PR8/34) or His-FPV-NP (A/FPV/Bratislawa/79) were mixed and assayed (30 nM each protein) for interactions *in vitro* using the Alpha screen technology. As a negative control GST alone was incubated with His-PR8-NP. The interaction of GST-UAP56 and His-PR8-NP was set to 100% as a reference for the other interactions.

described above but with GSH replaced with 250 mM imidazole), and dialyzed against elution buffer without imidazole.

Alpha screen. The Alpha screen assay (Perkin-Elmer) was performed with a 384-well OptiPlate with a 25-μl reaction mixture volume. The recombinant proteins were incubated for 2 h at room temperature at a final concentration of 30 nM each protein in Alpha screen buffer (PBS [pH 7.2], 0.1% BSA), together with AlphaLISA anti-GST acceptor beads and Alpha screen Ni-chelate donor beads at a concentration of 20 μg/ml. Interactions were analyzed with a Perkin-Elmer Envision device.

Real-time PCR. pCMV-UAP56 was a gift from C. Basler and P. Palese (New York, NY). UAP56 was cloned into pcDNA3.1 (Invitrogen) with primers containing an N-terminal FLAG tag (forward primer CGAATTGGATCCGCCAC CATGGACTACAAAGACGATGACGATAAAGCAGAGAACGATGT GGAC and reverse primer GGATGACTCGAGGGGCGAGTCTTCTACCGT GTCTGTTCAATGTAGGAGG). FLAG-URH49 was a gift from P. Lischka (Erlangen, Germany). Nucleoproteins of PR8 and FPV were cloned into pcDNA3.1. RNA was isolated as previously described (25). Reverse transcription was performed by using Superscript III (Invitrogen) according to the manufacturer's protocol, using either an oligo(dT) primer or a sequence-specific primer (18S rRNA) and 1 μg RNA. qPCR was carried out by using Eva-Green ready-to-use qPCR mix (Biotium) and primers specific for FPV-M1, FPV-M2, FPV-NP, FPV-NS1, FPV-HA, and 18S rRNA on a Applied Biosystems 7300 qPCR cycler (40 cycles of 10 s at 95°C, 20 s at 55°C, and 27 s at 72°C). For the 18S rRNA control, reverse transcription was performed with an 18S rRNA-specific primer. Sequence Detection software 1.4 was used to analyze the data. The following primers were used: M1 for (GACCAATCCTGTCACCTC), M1 rev (GATCCC CGTTCCCATTAAGGG), M2 for (GAGGTCGAAACGCCTAT), M2 rev (CT CCAAGCTCTATGCTGACAAA), NP for (TGTGCAACATCCTCAAAGGA AA), NP rev (GAGCCACTGATCCCCTCAGA), NS1 for (CATGCTCATGC CCAAACAGA), NS1 rev (TCCTCGGTGAAAGCCCTTAG), HA for (GCAG GTTGATGCCAATTGC), HA rev (TTCATCCCTGTTGCCAATAATAGA), 18S rRNA for (CAAGACGGACCAGAGCGAAA), and 18S rRNA rev (GGC GGGTCATGGGAATAAC).

Northern blotting. Northern blot analysis was performed as previously described (25). Ten micrograms of nuclear or cytoplasmic RNA was loaded per lane. After the transfer of the separated RNAs onto nylon membranes, the RNA was UV cross-linked by using a UV Stratalinker 1800 instrument (Stratagene). Before hybridization the blots were stained with methylene blue in 0.3 M sodium acetate (pH 5.0) to visualize precursor 28S rRNA and 18S RNA. Hybridization was carried out with digoxigenin (DIG)-labeled negative-stranded RNA probes for NP and M by using the Northern Starter kit (Roche) according to the manufacturer's instructions. The RNA probes were *in vitro* transcribed from linearized plasmid templates containing the M and NP segments of FPV. The Northern blots were analyzed with a Fuji imager. Bands representing M1 mRNA, NP mRNA, or 18S rRNA were quantified by using Multi Gauge 3.0 software.

RESULTS

The overall goal of our study was to dissect the role of UAP56 in the course of influenza A virus replication. Since all human cells express both UAP56 and its paralog URH49, it was pivotal to monitor the effects of both helicases on influenza A virus infection. First, we tested whether both URH49 and UAP56 would interact with NP from human and/or avian influenza A virus strains. To this end, NP from human influenza virus strain A/PR/8/34 or avian influenza virus strain A/Bratislawa/79/H7N7 was coexpressed with FLAG-tagged human UAP56 or URH49 in human HEK 293T cells. UAP56 or URH49 was then immunoprecipitated, and the associated proteins were analyzed by Western blotting. Interestingly, the NPs from both the human and avian influenza virus strains were capable of forming a complex with UAP56 as well as URH49 (Fig. 1A).

The direct protein interaction between avian or human NP and URH49 as well as UAP56 was confirmed *in vitro* by using the Alpha screen technique. The data show that *in vitro*, URH49 and UAP56 interacted with an affinity similar to that of NP derived from a human or an avian influenza A virus strain (Fig. 1B).

Influence of URH49 or UAP56 knockdown on viral titers. We next tested whether the individual knockdown of URH49 or UAP56 would affect the efficiency of avian and human influenza A virus replication. For this purpose A549 cells were first transfected with pools of siRNAs specific for either URH49 or UAP56. The knockdown of the targeted proteins was verified by Western blot analysis (Fig. 2A). Importantly, the transfection of the siRNAs did not upregulate the expression of the type I interferon (IFN)-inducible MxA protein (1, 36), demonstrating that type I IFN was not induced by the application of the siRNAs used in this study (Fig. 2A). The depletion of URH49 or UAP56 in A549 cells with specific siRNAs strongly affected the replication efficiency of both human and avian influenza A viruses (Fig. 2B to D). The knockdown of UAP56 and URH49 led to reductions of avian influ-

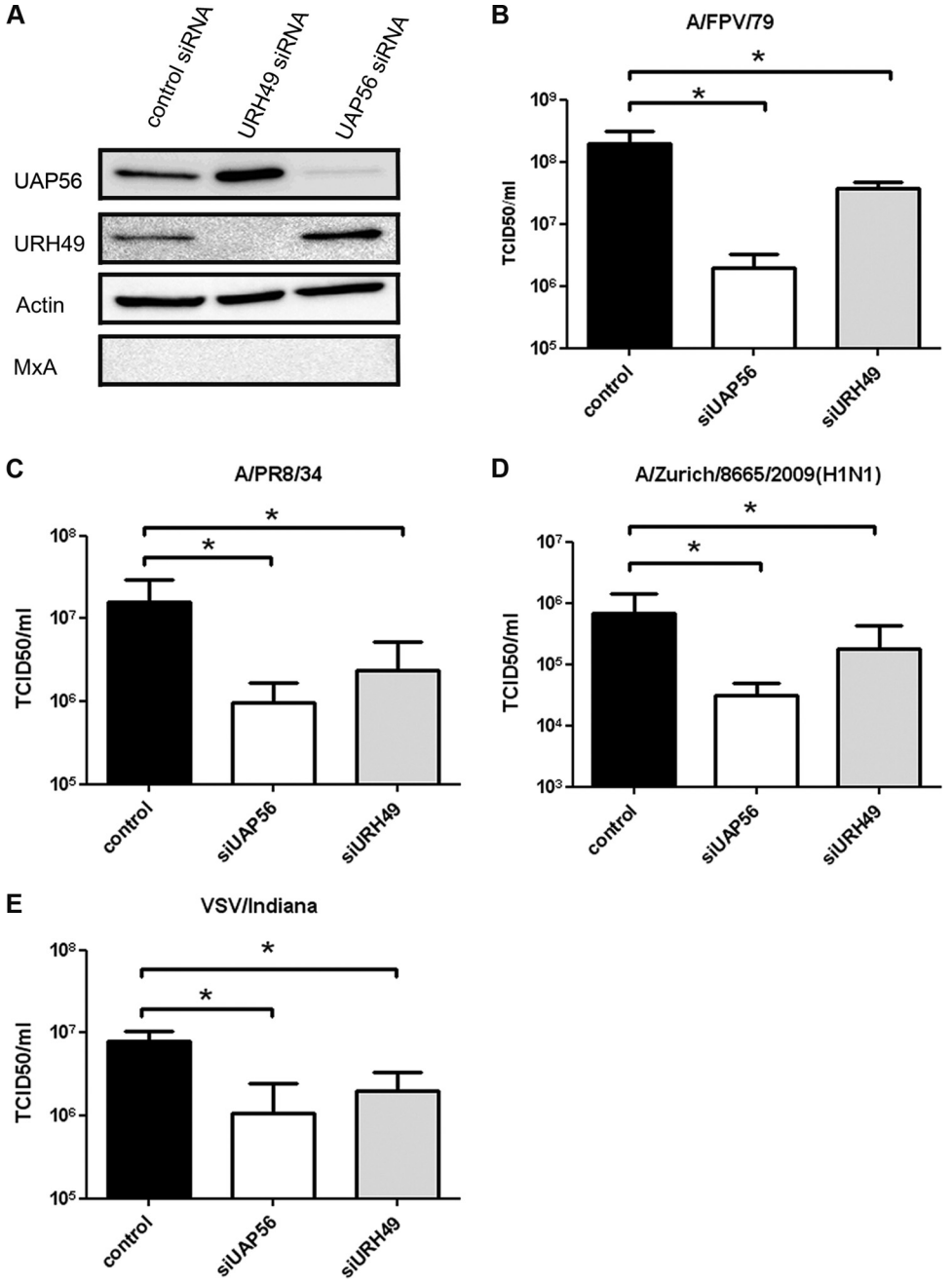

FIG. 2. Knockdown of UAP56 or URH49 results in a strong reduction of titers of influenza A virus. (A) A549 cells were treated with the indicated siRNAs for 48 h. Protein levels of UAP56 and URH49 were analyzed by Western blotting. MxA was used to monitor the induction of interferon in siRNA-treated cells. (B to E) A549 cells were treated with the indicated siRNAs for 48 h and subsequently infected with FPV (MOI = 0.1) (B), PR8 (MOI = 0.1) (C), A/Zurich/8665/2009(H1N1) (MOI = 1) (D), and VSV Indiana (MOI = 0.1) (E), and culture supernatants were taken 24 h postinfection and assayed for virus titers by using the $TCID_{50}$ method. For VSV, virus titers were measured after 12 h. An asterisk indicates a P value of <0.05.

enza virus A/FPV/79 titers by factors of 200 and 5, respectively (Fig. 2B). Less pronounced but still significant reductions ($P < 0.05$) of viral titers were observed with laboratory strain A/PR/8/34, where the downregulations of UAP56 and URH49 led to 20- and 5-fold decreases of viral titers, respectively (Fig. 2C). Similarly, we observed significant ($P < 0.05$) 5- and 50-fold titer reductions in UAP56- and URH49-depleted cells, respectively, infected with a Zürich isolate of the pandemic H1N1 influenza virus (Fig. 2D). Surprisingly, infection with VSV also led to significant ($P < 0.05$) 5- and 9-fold reductions of titers at 12 h postinfection in UAP56 and URH49 knockdown cells, respectively (Fig. 2E). To exclude the remote possibility that the observed reduction of influenza A virus titers in A549 cells depleted of URH49 or UAP56 was due simply to the induction

of type I interferon by siRNA treatment, we repeated the experiment with transfected A549 cells stably expressing the V protein of simian virus 5 (SV5) (see Fig. S1 in the supplemental material). The V protein is a potent inhibitor of the type I IFN-mediated expression of type I IFN-induced effector proteins (7). As expected, A549 cells stably expressing the V protein were no longer capable of synthesizing MxA upon induction with saturating amounts of IFN-α2 (Fig. S1D). Nevertheless, in these cells, titers of avian influenza A virus were reduced to the same extent as that in A549 wild-type cells when either URH49 or UAP56 was depleted (Fig. S1A, S1B, and S1C), indicating that the observed reductions in titers were not simply the result of a type I interferon-mediated antiviral response.

Influence of URH49 or UAP56 knockdown on splicing and nuclear export of viral mRNAs. To better define the step(s) of the influenza A virus replication cycle affected by the depletion of URH49 or UAP56, we examined the splicing and nuclear export of viral mRNAs of segment 7 (M segment). Read and Digard recently showed that UAP56 plays a role in the nuclear export of several human influenza A virus mRNAs, namely, M1, M2, NS1, and HA mRNAs, while the export of other viral mRNAs, in particular NP mRNA, was largely independent of UAP56 (28). A549 cells depleted of URH49 or UAP56 were infected at an MOI of 5 with avian influenza A virus for 4 h. RNA isolated from the nuclear and cytoplasmic fractions was then analyzed either by Northern blotting (Fig. 3A) using negative-stranded RNA probes specific for NP and M or by qPCR (Fig. 3B) using primers specific for M1, NP, HA, and NS1 or primers specific for unspliced M1 mRNA and spliced M2 mRNA (Fig. 3E). Northern blot analysis revealed that in cells transfected with control siRNA, both the mRNAs coding for NP and M1 accumulated primarily in the cytoplasm (approximately 60%) (Fig. 3A, C, and D). In contrast, the depletion of UAP56 or URH49 reduced the nuclear export of the NP and M1 RNAs to the cytoplasm. The knockdown of URH49 limited the accumulation of NP mRNA and M1 mRNA to 38% and 43%, respectively (Fig. 3A, C, and D). Although the depletion of UAP56 had a less pronounced effect on the nuclear export of NP and M1 mRNAs, the data clearly indicate that both helicases are involved in this process. mRNAs encoding M2 were not detectable by Northern blotting. When the RNA samples were analyzed by qPCR, similar results were obtained (Fig. 3B). The data are shown as means of data from 5 independent experiments, each normalized to 18S rRNA data. The depletion of URH49 led to a reduced export of M1 and NP mRNAs into the cytoplasm (18% M1 mRNA and 19% NP mRNA in the cytoplasm) compared to treatment with control siRNA (37% M1, 28% NP, 36% HA, and 23% NS1 mRNAs in the cytoplasm), while the nuclear export of HA mRNA was only marginally affected (33% HA mRNA in the cytoplasm), and that of NS1 was even enhanced (40% NS1 mRNA in the cytoplasm). The knockdown of UAP56 reduced the export of the mRNAs encoding M1, HA, and NS1 (25% M1, 23% HA, and 19% NS1 mRNAs in the cytoplasm) but had only a marginal effect on NP mRNA export (24% NP RNA in the cytoplasm). Furthermore, the depletion of URH49 or UAP56 had no effect on the ratio between unspliced M1 and spliced M2 mRNAs in the nuclear or cytoplasmic RNA fraction (Fig. 3E). The spliced M2 RNA accumulated to approximately 5% of the amount of M1 mRNA, suggesting that the splicing of the M segment does not require the activity of URH49 or UAP56. However, we cannot exclude the possibility that UAP56 and URH49 has an overlapping function in the assembly of the cellular splicing complex. Taken together, URH49 and, to a certain extent, UAP56 play a role in the nuclear export of viral mRNAs. However, the partial nuclear retention of viral mRNAs in UAP56-depleted cells clearly does not explain the strong (200-fold) reduction of FPV titers in these cells.

Activation of dsRNA-dependent PKR. Both UAP56 and URH49 were previously shown to exhibit RNA helicase (unwinding) activity (35, 37). It is therefore conceivable that URH49 and/or UAP56 plays a role in the prevention of the generation of detectable dsRNA replicative intermediates during influenza A virus replication/transcription. In contrast to positive-strand RNA viruses, negative-strand RNA viruses do not appear to produce detectable amounts of viral dsRNA intermediates in infected cells (39). In order to address this question, we tested the accumulation of dsRNA by monitoring the phosphorylation of dsRNA-dependent protein kinase R (PKR). The binding of dsRNAs of more than 30 bp in length leads to the activation of latent PKR by dimerization and autophosphorylation (29). A549 cells depleted of URH49 or UAP56 were either mock infected or infected with human and avian influenza A viruses for 4 h. Protein extracts of these cells were analyzed by Western blotting using a phospho-PKR-specific antibody (Fig. 4A). The data (Fig. 4C and D) revealed that the depletion of URH49 or UAP56 resulted in a partial activation of PKR. Moreover, influenza A virus infection of cells treated with siRNA specific for URH49 or UAP56 strongly enhanced the activation of PKR. In contrast, no activation of PKR was evident in mock-infected control siRNA-treated cells, and only a weak activation was observed upon infection (Fig. 4C). In addition, immunostaining of M1 revealed a strong reduction of M1 protein expression levels in UAP56- or URH49-depleted cells that paralleled the observed reduction in virus yield (Fig. 2B and C). Taken together, these observations indicate that URH49 and UAP56 do indeed play a role in preventing the accumulation of dsRNA in virus-infected cells. In addition, we also tested whether the depletion of URH49 and UAP56 would result in the synthesis of type I interferon. This was not the case, since we did not observe an activation of the transcription factor interferon regulatory factor 3 (IRF3) or the secretion of beta interferon by URH49- or UAP56-depleted cells, independent of whether they were infected or not (data not shown).

Accumulation of dsRNA in UAP56-depleted cells. The observed activation of PKR in URH49- or UAP56-depleted cells infected with influenza A virus could be the result of an accumulation of dsRNA. To address this, we took advantage of a monoclonal antibody highly specific for dsRNA. Weber and colleagues (39) previously showed that infection with positive-stranded but not negative-stranded RNA viruses, such as influenza virus, resulted in the accumulation of virus-specific dsRNA in host cells. We infected A549 cells following treatment with either control siRNA or siRNA specific for URH49 or UAP56 with avian (Fig. 5A) or human (Fig. 5B) influenza A virus for 4 h, representing the optimal time frame for allowing dsRNA formation. As expected, in control siRNA-treated cells, infection with influenza virus did not yield detectable

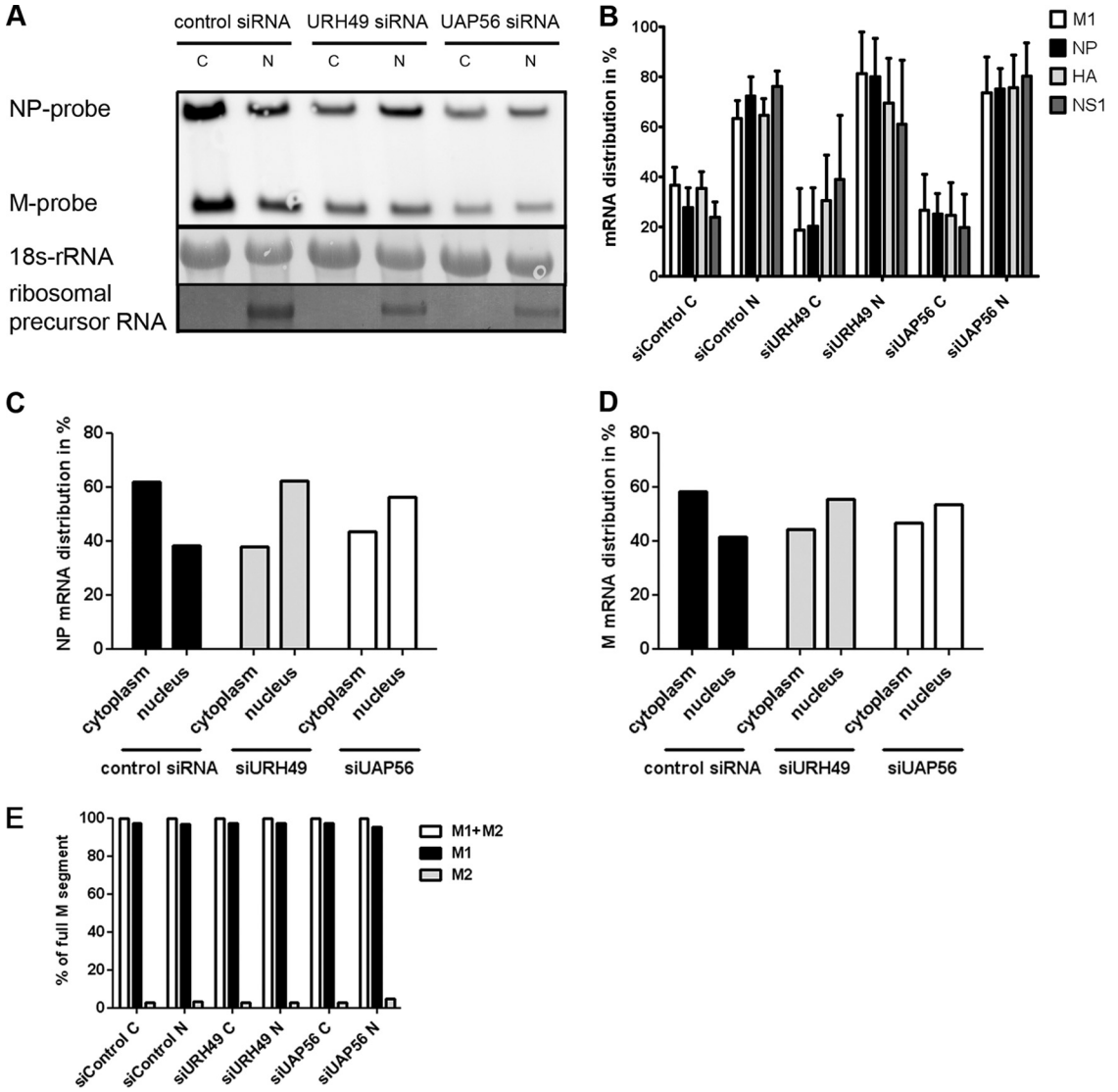

FIG. 3. Reduced export of viral mRNAs in cells treated with UAP56- or URH49-specific siRNA upon infection with influenza A virus. (A) A549 cells were treated with the indicated siRNA for 72 h and subsequently infected with FPV for 4 h (MOI = 5). Cytoplasmic and nuclear RNAs were isolated, and 5 μg of RNA per lane was analyzed by Northern blotting. Methylene blue-stained 18S rRNA was used to normalize the total amounts of RNA in each lane. Precursor rRNA was detectable only in the nuclear RNA fraction. The separated RNAs were hybridized with DIG-labeled probes specific for influenza A virus M and NP segments. (B) Reverse transcription was performed with cytoplasmic and nuclear RNA using an oligo(dT) primer and 1 μg RNA. M1, NP, HA, and NS1 levels in the two subcellular fractions were analyzed by qPCR using specific primer pairs for the indicated viral mRNAs; results are shown as means of data from five independent experiments. (C and D) The nuclear or cytoplasmic localizations of NP (C) and M1 (D) mRNAs in A were quantified by measuring band intensities using Multi Gauge software from Fujifilm. Total mRNA from the cytoplasmic and nuclear fractions of control siRNA-treated cells was set as the reference. (E) Splicing of the influenza A virus M segment was not affected by the knockdown of UAP56 or UARH49. Reverse transcription was performed from cytoplasmic and nuclear RNAs using the oligo(dT) primer and 1 μg RNA. M1 and M2 levels were assessed by real-time qPCR using specific primer pairs for M1 and M2.

levels of dsRNA (Fig. 5A and B). In contrast, infection of UAP56-depleted cells led to a pronounced accumulation of dsRNA in the perinuclear space (Fig. 5A and B). Notably, the depletion of URH49 did not result in the accumulation of dsRNA in the infected cells despite the fact that we observed a pronounced activation of PKR in these cells (Fig. 4C). Mock infection of URH49- or UAP56-depleted cells yielded much lower levels of dsRNA, suggesting that the observed dsRNA was predominantly of viral origin (Fig. 5C). The puzzling observation of the perinuclear accumulation of dsRNA raised the possibility that the antibody detected incoming RNPs in a panhandle conformation (17) that may require unwinding before passage through the nuclear pore. To test this hypothesis, we treated the cells with actinomycin D before infection, thereby preventing *de novo* synthesis and nuclear export of viral RNAs (38). Evidently, the inhibition of viral RNA synthesis strongly reduced the accumulation of dsRNA in UAP56-depleted cells. Nevertheless, small amounts of dsRNA located in the cytoplasm were detectable in UAP56-depleted and, surprisingly, also in URH49-depleted cells (Fig. 6A). The fact that

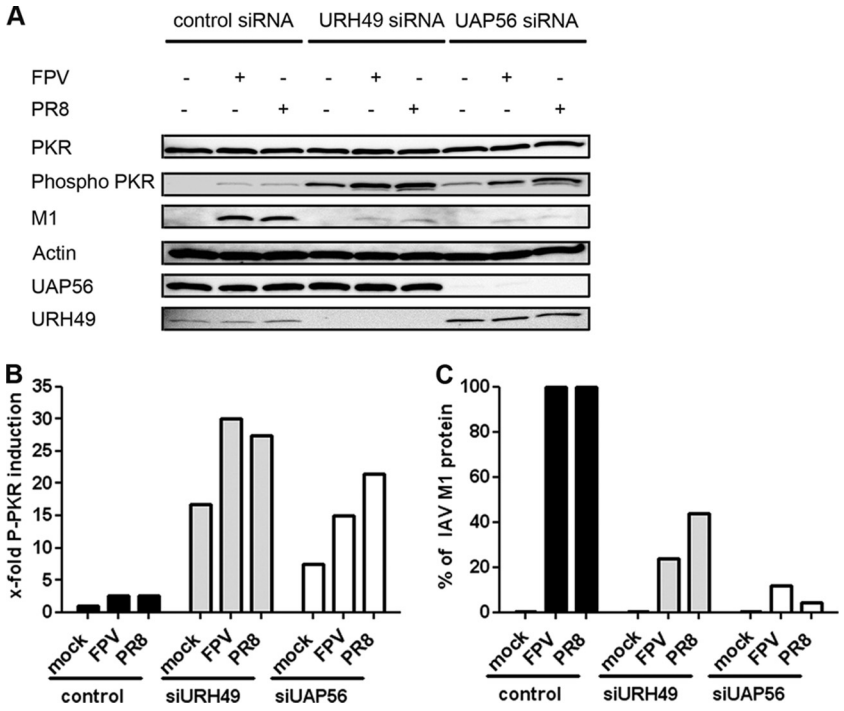

FIG. 4. PKR is phosphorylated in UAP56 and URH49 knockdown cells upon infection with influenza A virus. (A) A549 cells were treated with 30 nM the indicated siRNAs for 72 h and subsequently infected with influenza virus PR8 or FPV for 4 h (MOI = 5). Total cell lysates were analyzed by Western blotting using specific antibodies against PKR, phospho-PKR, influenza virus M1, actin, UAP56, and URH49. (B and C) Phospho-PKR levels (B) and influenza virus M1 protein levels (C) were quantified by measuring band intensities using Multi Gauge software from Fujifilm.

dsRNA accumulated very early in the infection cycle prompted us to test whether primary transcription by the virion-associated polymerase complex (in the absence of the synthesis of viral proteins) would provide sufficient amounts of viral RNA. This was clearly not the case; the pretreatment of URH49- or UAP56-depleted cells with cycloheximide prevented the accumulation of dsRNA (Fig. 6B). Controls with mock-infected cells showed only very small amounts of dsRNA cells depleted of UAP56 or URH49 (Fig. 5C and see Fig. S2A and S2B in the supplemental material). Interestingly, treatment with leptomycin B, which blocks the nuclear export of vRNPs into the cytoplasm, did not prevent the accumulation of dsRNA in the perinuclear region of UAP56-depleted cells infected with FPV, suggesting that the observed dsRNA does not consist of mature vRNA (Fig. S3).

In order to assess whether the observed activity of UAP56 or URH49 may also apply to other negative-strand viruses, we infected URH49- or UAP56-depleted A549 cells with VSV and looked for the accumulation of dsRNA using the dsRNA-specific antibody. Intriguingly, similarly to influenza A virus infection, dsRNA accumulated to high levels in the perinuclear region of UAP56-depleted cells, whereas dsRNA was not detectable in URH49 siRNA- or control siRNA-treated cells (Fig. 7).

DISCUSSION

UAP56 has been shown to link mRNA transcription and splicing to the nuclear export of cellular RNA. Although encoded by two distinct genes, the RNA helicases UAP56 and URH49 show an identity of 90% at the amino acid level (27). There is increasing evidence that UAP56 is involved in the nuclear export of influenza virus mRNAs (2, 28, 38). This raises the question of whether or not URH49 may also play a role in the transcription/replication of influenza A viruses. Coimmunoprecipitation and Alpha screen assays have demonstrated that URH49 is capable of binding NP from both avian and human influenza A viruses and does so with an efficiency similar to that of UAP56 (Fig. 1). However, when we analyzed the functions of URH49 and UAP56 in the replication of avian and human influenza viruses, it became evident that only UAP56 was required for the efficient replication of avian influenza virus (Fig. 2B), while both URH49 and UAP56 showed an intermediate effect on human influenza A virus. A possible explanation for these observations is that for human influenza virus, the two helicases exert a partially overlapping function. In this context, it is interesting that the depletion of URH49 or UAP56 always resulted in an increased expression level of the paralogous helicase (Fig. 2A). Scans of the chicken genome database for UAP56 and URH49 revealed the presence of only the gene homologs of UAP56. Hence, it is conceivable that human URH49 may only partially complement the activity of UAP56 in conjunction with the avian influenza A virus replication/transcription machinery.

Several previous studies have shown that the export of spliced as well as unspliced influenza virus mRNAs encoding late viral proteins is at least partially dependent on NFX1 and UAP56 (2, 13, 28, 38). In contrast, the nuclear export of unspliced mRNAs encoding early gene products, such as PB2 or NP, appears to be largely independent of UAP56 viral mRNAs

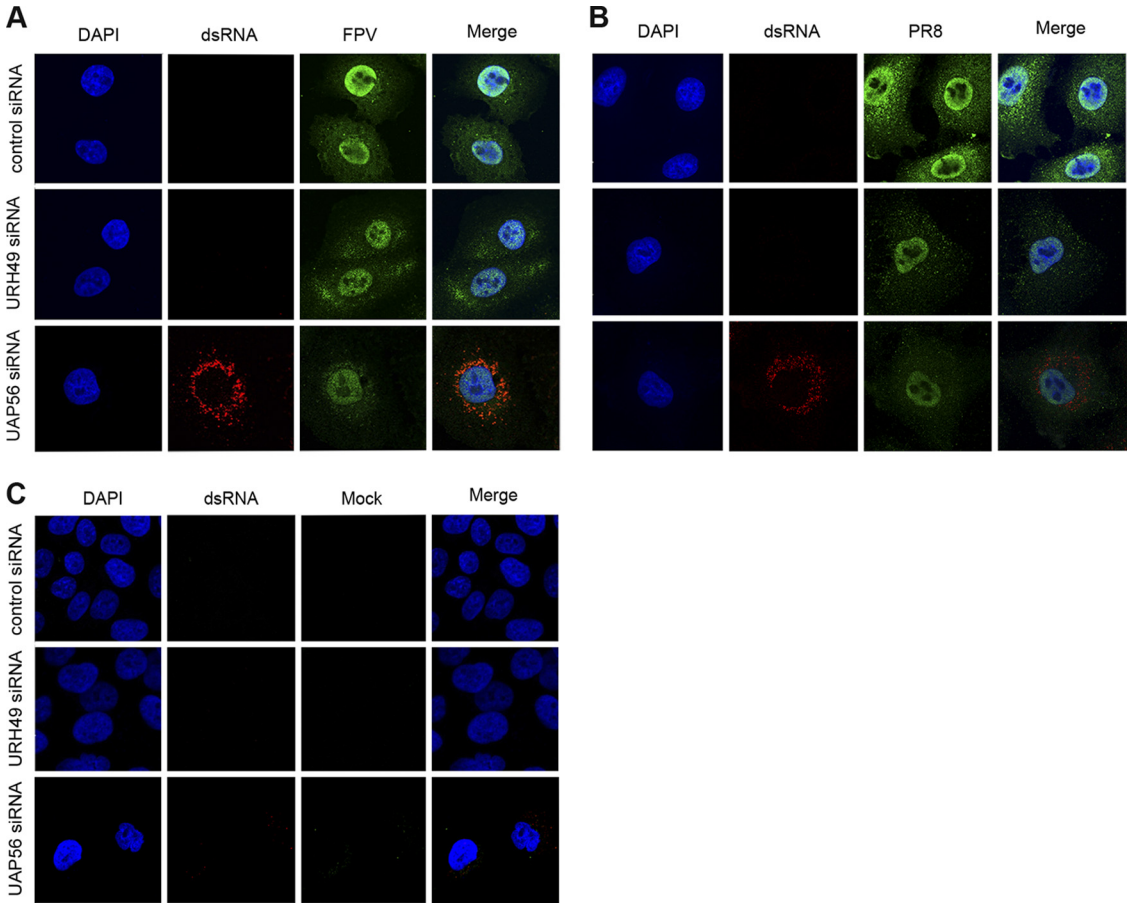

FIG. 5. dsRNA accumulates in the perinuclear region of UAP56 knockdown cells infected with human or avian influenza A virus. A549 cells were treated with the indicated siRNAs for 72 h and infected with FPV (A) or PR8 (B) for 4 h or mock infected (C). Cells were fixed with 4% formaldehyde and permeabilized with 0.5% Triton X-100. Cells were stained by using an anti-influenza virus serum (1:300) and anti-dsRNA antibody (1:3,000). Pictures were taken with a Leica TCS-SP5 confocal microscope.

(28). Hence, whereas the nuclear export of mRNAs encoding M1, HA, and NS1 depended partially on the function of UAP56, the nuclear export of NP mRNA was only marginally reduced in UAP56-depleted cells. Surprisingly, however, the nuclear export of NP mRNA was at least partially dependent on the presence of URH49 (Fig. 3A and B). Our data thus demonstrate that URH49 is also involved in the nuclear export of viral mRNA, providing further support to the notion that URH49 exerts a function similar to that UAP56 although forming distinct nuclear export complexes (41). In addition, our data provide clear evidence that neither UAP56 nor URH49 is required for the splicing of M2 mRNA (Fig. 3E).

The fact that during the transcription/replication of negative-stranded RNA viruses, including influenza virus, dsRNA intermediates are not detectable (39) suggests the involvement of cellular RNA helicases. Hence, the association of UAP56 with vRNPs (19) may be crucial not only for the nuclear export of viral mRNA but also for the prevention of the formation of dsRNA replicative intermediates. The presence of dsRNA in infected cells plays a pivotal role in triggering the type I interferon response (12). This hypothesis prompted us to test whether the depletion of UAP56 or URH49 (i) results in the accumulation of dsRNA and (ii) would lead to the activation of dsRNA-dependent PKR. Since PKR is localized in the cytoplasm, its pronounced activation in UAP56- or URH49-depleted cells pointed to the accumulation of dsRNA in the cytoplasm. Immunostaining of dsRNA using a specific antibody revealed that, at least for UAP56, this was indeed the case (Fig. 5). Infection of UAP56-depleted cells with avian and human influenza A viruses or VSV invariably led to the accumulation of dsRNA in the perinuclear region (Fig. 4 and 6), thus providing an explanation for the activation of PKR. However, in the case of URH49 depletion, it is not clear why no dsRNA was detectable despite the pronounced activation of PKR in these cells. A possible explanation for this finding may be that only small amounts of dsRNA were produced, which were sufficient for the activation of PKR but not detectable by the anti-dsRNA antibody. The fact that the depletion of UAP56 and URH49 led to a modest activation of PKR in mock-infected cells is puzzling (Fig. 4A). It is conceivable that during the nuclear export of cellular mRNAs, the unwinding activity of UAP56 is required to prevent the cytoplasmic accumulation of highly structured mRNAs capable of inducing the activation of PKR.

Recently, Burgui and colleagues showed that the influenza virus polymerase complex remains associated with the cap

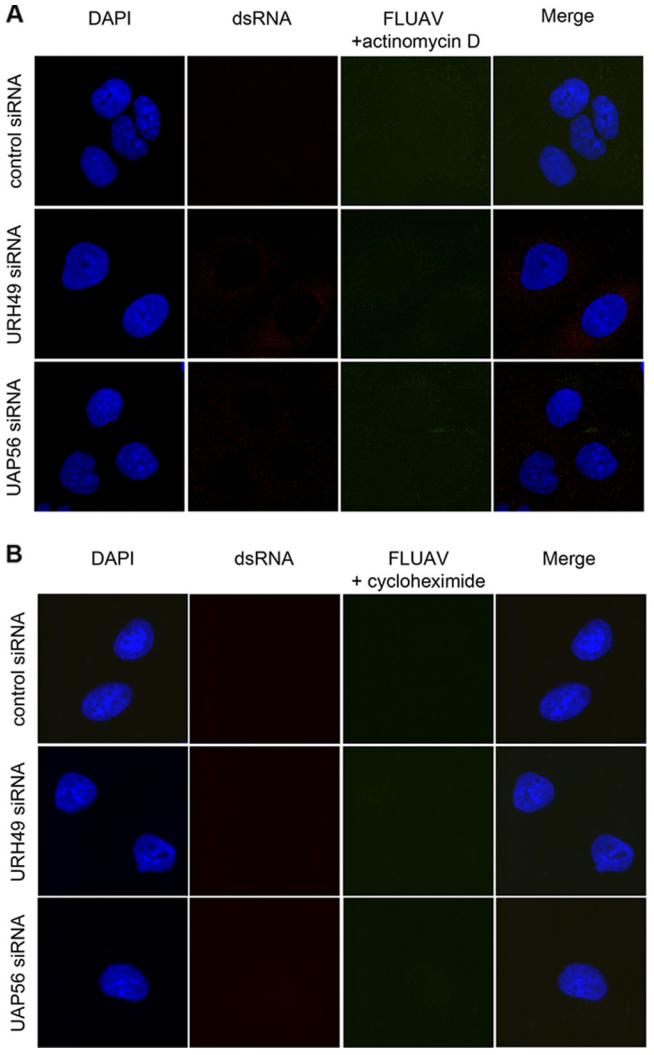

FIG. 6. Treatment with cycloheximide or actinomycin D prevents accumulation of dsRNA in UAP56-depleted cells infected with influenza A virus. A549 cells were treated with the indicated siRNAs for 72 h. Cells were incubated with actinomycin D (0.5 μg/ml) (A) or cycloheximide (75 μg/ml) (B) 1 h before infection. Cells were infected with FPV (MOI = 5). Inhibitors remained in the medium during and after infection. Cells were fixed at 4 h postinfection and stained by using an anti-influenza virus serum (1:300) and anti-dsRNA antibody (1:3,000). Pictures were taken with a Leica TCS-SP5 confocal microscope.

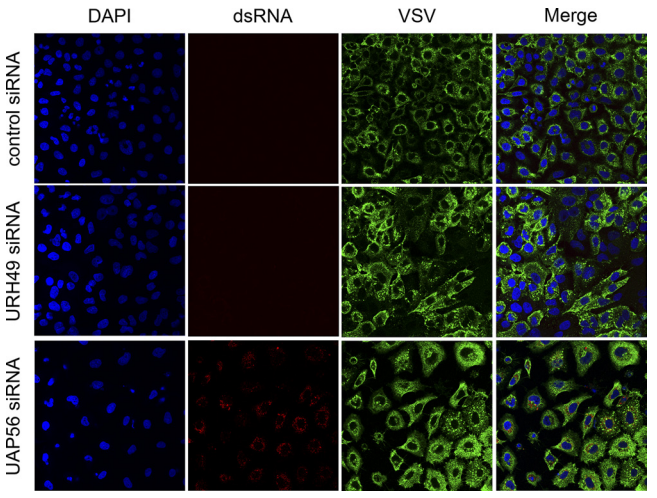

FIG. 7. Vesicular stomatitis virus induces accumulation of dsRNA in UAP56 knockdown cells. (A) A549 cells were treated with the indicated siRNAs for 72 h and subsequently infected with VSV Indiana for 4 h. Cells were fixed with 4% formaldehyde and permeabilized with 0.5% Triton X-100. Cells were stained by using a polyclonal anti-VSV serum (1:300) and anti-dsRNA antibody (1:3,000). Pictures were taken with a Leica TCS-SP5 confocal microscope.

structure of the viral mRNA in the cytoplasm, replacing the function of the cellular factor eukaryotic initiation factor 4E (eIF4E) (3). Hence, it is tempting to speculate that UAP56 remains associated with the viral mRNA via the polymerase complex, facilitating the translation of the viral mRNA. Indeed, a function similar to the activity of eIF4A in protein translation was recently shown for UAP56 in cardiomyocytes (30). So far, a defined activity in the cytoplasm has been demonstrated only for UAP56 (20, 31).

Although it is highly likely that the observed dsRNA is predominantly of viral origin, we have no formal proof. Nevertheless, the inhibition of replication with actinomycin D or cycloheximide (allowing primary transcription) abrogated the formation of dsRNA. Recently, Dauber and colleagues showed that in the absence of a functional NS1 protein, cytoplasmic vRNPs are capable of inducing dsRNA-dependent PKR during the late phase of influenza B virus infection (5). Incidentally, B/NS1 was reported previously to colocalize with several factors of the nuclear export machinery in nuclear speckles and to interact with UAP56 *in vitro* (32). However, the inhibition of the CRM-1-mediated nuclear export of vRNPs by treatment with leptomycin (8) had no effect on the accumulation of dsRNA (see Fig. S3 in the supplemental material), strongly suggesting that the accumulating dsRNA in the perinuclear region does not consist of vRNPs.

There is ample evidence that the NS1 protein of influenza viruses efficiently interferes with the activation of PKR (reviewed in references 11 and 40). Hence, the observed activation of PKR in influenza virus-infected cells lacking either UAP56 or URH49 could be due to low levels of NS1. The nuclear export of NS1 mRNA is reduced in cells depleted of UAP56 (28) or URH49 (data not shown). However, despite a pronounced activation of PKR, the depletion of UAP56 or URH49 did not result in the production of detectable amounts of type I interferons in the culture supernatants of influenza virus-infected cells, nor did we observe an activation of IRF3 (data not shown). Hence, it is conceivable that the observed inhibition of the interferon signaling cascade is due to the activity of low levels of NS1 interfering with the activation of RIG-I (10, 40), suggesting that the reduced amount of NS1 is still sufficient for interfering with the type I interferon response. In this context, it is interesting that Ostertag and colleagues reported previously that the infection of host cells with a polR mutant of VSV (containing a single-amino-acid substitution in the N protein) resulted in the overproduction of viral dsRNA and, as a consequence, the activation of PKR. Surprisingly, however, the observed growth restriction of this mutant virus was independent of the type I interferon response (23,

24). Hence, it would be interesting to test whether the observed growth restriction phenotype of this VSV polR mutant could be linked to the activity of UAP56.

It is intriguing that influenza virus-induced dsRNA was not observed in the nuclei of UAP56- or URH49-depleted cells (Fig. 5). Since influenza viruses replicate in the host cell nucleus, we would have expected an accumulation of dsRNA primarily in the nucleus. One possible explanation is that URH49 and UAP56 may be able to complement their unwinding activity in the nucleus. Unfortunately, it is not possible to test this hypothesis, since the concomitant depletion of URH49 and UAP56 led to cell death within 72 h of the start of siRNA treatment (data no shown; see also references 14 and 15).

Taken together, we were able to show that the cellular RNA helicases UAP56 and URH49 not only play a role in the nuclear export of viral RNA but also are required to prevent the activation of PKR. Moreover, UAP56 prevents the formation of virus-induced dsRNA and, hence, the antiviral response of PKR in influenza virus- and VSV-infected cells. Moreover, it will be interesting to elucidate whether the usurpation of the activity of UAP56 may be a general viral strategy for evading the innate immune system.

ACKNOWLEDGMENTS

We thank Alexandra Trkola, Anders Krarup, and Axel Mann for helpful discussions. The cDNA for UAP56 was kindly provided by C. Basler and P. Palese. The FLAG-URH49 expression construct was kindly provided by T. Stamminger.

This work was supported by a grant from the Swiss National Science Foundation.

REFERENCES

1. **Aebi, M., et al.** 1989. cDNA structures and regulation of two interferon-induced human Mx proteins. Mol. Cell. Biol. **9:**5062–5072.
2. **Amorim, M. J., E. K. Read, R. M. Dalton, L. Medcalf, and P. Digard.** 2007. Nuclear export of influenza A virus mRNAs requires ongoing RNA polymerase II activity. Traffic **8:**1–11.
3. **Burgui, I., E. Yanguez, N. Sonenberg, and A. Nieto.** 2007. Influenza virus mRNA translation revisited: is the eIF4E cap-binding factor required for viral mRNA translation? J. Virol. **81:**12427–12438.
4. **Carmody, S. R., and S. R. Wente.** 2009. mRNA nuclear export at a glance. J. Cell Sci. **122:**1933–1937.
5. **Dauber, B., et al.** 2009. Influenza B virus ribonucleoprotein is a potent activator of the antiviral kinase PKR. PLoS Pathog. **5:**e1000473.
6. **Dias, A., et al.** 2009. The cap-snatching endonuclease of influenza virus polymerase resides in the PA subunit. Nature **458:**914–918.
7. **Didcock, L., D. F. Young, S. Goodbourn, and R. E. Randall.** 1999. The V protein of simian virus 5 inhibits interferon signalling by targeting STAT1 for proteasome-mediated degradation. J. Virol. **73:**9928–9933.
8. **Elton, D., et al.** 2001. Interaction of the influenza virus nucleoprotein with the cellular CRM1-mediated nuclear export pathway. J. Virol. **75:**408–419.
9. **Fleckner, J., M. Zhang, J. Valcarcel, and M. R. Green.** 1997. U2AF65 recruits a novel human DEAD box protein required for the U2 snRNP-branchpoint interaction. Genes Dev. **11:**1864–1872.
10. **Gack, M. U., et al.** 2009. Influenza A virus NS1 targets the ubiquitin ligase TRIM25 to evade recognition by the host viral RNA sensor RIG-I. Cell Host Microbe **5:**439–449.
11. **Hale, B. G., R. E. Randall, J. Ortin, and D. Jackson.** 2008. The multifunctional NS1 protein of influenza A viruses. J. Gen. Virol. **89:**2359–2376.
12. **Haller, O., G. Kochs, and F. Weber.** 2006. The interferon response circuit: induction and suppression by pathogenic viruses. Virology **344:**119–130.
13. **Hao, L., et al.** 2008. Drosophila RNAi screen identifies host genes important for influenza virus replication. Nature **454:**890–893.
14. **Hautbergue, G. M., et al.** 2009. UIF, a new mRNA export adaptor that works together with REF/ALY, requires FACT for recruitment to mRNA. Curr. Biol. **19:**1918–1924.
15. **Kapadia, F., A. Pryor, T. H. Chang, and L. F. Johnson.** 2006. Nuclear localization of poly(A)+ mRNA following siRNA reduction of expression of the mammalian RNA helicases UAP56 and URH49. Gene **384:**37–44.
16. **Lamb, R. A., and C. M. Horvath.** 1991. Diversity of coding strategies in influenza viruses. Trends Genet. **7:**261–266.
17. **Luo, G. X., W. Luytjes, M. Enami, and P. Palese.** 1991. The polyadenylation signal of influenza virus RNA involves a stretch of uridines followed by the RNA duplex of the panhandle structure. J. Virol. **65:**2861–2867.
18. **Luo, M. L., et al.** 2001. Pre-mRNA splicing and mRNA export linked by direct interactions between UAP56 and Aly. Nature **413:**644–647.
19. **Mayer, D., et al.** 2007. Identification of cellular interaction partners of the influenza virus ribonucleoprotein complex and polymerase complex using proteomic-based approaches. J. Proteome Res. **6:**672–682.
20. **Meignin, C., and I. Davis.** 2008. UAP56 RNA helicase is required for axis specification and cytoplasmic mRNA localization in Drosophila. Dev. Biol. **315:**89–98.
21. **Momose, F., et al.** 2001. Cellular splicing factor RAF-2p48/NPI-5/BAT1/UAP56 interacts with the influenza virus nucleoprotein and enhances viral RNA synthesis. J. Virol. **75:**1899–1908.
22. **Munoz, F. M., et al.** 2000. Current research on influenza and other respiratory viruses. II. International symposium. Antiviral Res. **46:**91–124.
23. **Ostertag, D., T. M. Hoblitzell-Ostertag, and J. Perrault.** 2007. Cell-type-specific growth restriction of vesicular stomatitis virus polR mutants is linked to defective viral polymerase function. J. Virol. **81:**492–502.
24. **Ostertag, D., T. M. Hoblitzell-Ostertag, and J. Perrault.** 2007. Overproduction of double-stranded RNA in vesicular stomatitis virus-infected cells activates a constitutive cell-type-specific antiviral response. J. Virol. **81:**503–513.
25. **Pavlovic, J., O. Haller, and P. Staeheli.** 1992. Human and mouse Mx proteins inhibit different steps of the influenza virus multiplication cycle. J. Virol. **66:**2564–2569.
26. **Pavlovic, J., T. Zurcher, O. Haller, and P. Staeheli.** 1990. Resistance to influenza virus and vesicular stomatitis virus conferred by expression of human MxA protein. J. Virol. **64:**3370–3375.
27. **Pryor, A., et al.** 2004. Growth-regulated expression and G0-specific turnover of the mRNA that encodes URH49, a mammalian DExH/D box protein that is highly related to the mRNA export protein UAP56. Nucleic Acids Res. **32:**1857–1865.
28. **Read, E. K., and P. Digard.** Individual influenza A virus mRNAs show differential dependence on cellular NXF1/TAP for their nuclear export. J. Gen. Virol. **91:**1290–1301.
29. **Sadler, A. J., and B. R. Williams.** 2007. Structure and function of the protein kinase R. Curr. Top. Microbiol. Immunol. **316:**253–292.
30. **Sahni, A., N. Wang, and J. D. Alexis.** 2010. UAP56 is an important regulator of protein synthesis and growth in cardiomyocytes. Biochem. Biophys. Res. Commun. **393:**106–110.
31. **Schmidt, U., et al.** 2009. Assembly and mobility of exon-exon junction complexes in living cells. RNA **15:**862–876.
32. **Schneider, J., B. Dauber, K. Melen, I. Julkunen, and T. Wolff.** 2009. Analysis of influenza B virus NS1 protein trafficking reveals a novel interaction with nuclear speckle domains. J. Virol. **83:**701–711.
33. **Shen, H.** 2009. UAP56—a key player with surprisingly diverse roles in pre-mRNA splicing and nuclear export. BMB Rep. **42:**185–188.
34. **Shen, H., et al.** 2008. Distinct activities of the DExD/H-box splicing factor hUAP56 facilitate stepwise assembly of the spliceosome. Genes Dev. **22:**1796–1803.
35. **Shen, J., L. Zhang, and R. Zhao.** 2007. Biochemical characterization of the ATPase and helicase activity of UAP56, an essential pre-mRNA splicing and mRNA export factor. J. Biol. Chem. **282:**22544–22550.
36. **Simon, A., J. Fah, O. Haller, and P. Staeheli.** 1991. Interferon-regulated Mx genes are not responsive to interleukin-1, tumor necrosis factor, and other cytokines. J. Virol. **65:**968–971.
37. **Sugiura, T., Y. Nagano, and Y. Noguchi.** 2007. DDX39, upregulated in lung squamous cell cancer, displays RNA helicase activities and promotes cancer cell growth. Cancer Biol. Ther. **6:**957–964.
38. **Wang, W., et al.** 2008. Imaging and characterizing influenza A virus mRNA transport in living cells. Nucleic Acids Res. **36:**4913–4928.
39. **Weber, F., V. Wagner, S. B. Rasmussen, R. Hartmann, and S. R. Paludan.** 2006. Double-stranded RNA is produced by positive-strand RNA viruses and DNA viruses but not in detectable amounts by negative-strand RNA viruses. J. Virol. **80:**5059–5064.
40. **Wolff, T., and S. Ludwig.** 2009. Influenza viruses control the vertebrate type I interferon system: factors, mechanisms, and consequences. J. Interferon Cytokine Res. **29:**549–557.
41. **Yamazaki, T., et al.** 2010. The closely related RNA helicases, UAP56 and URH49, preferentially form distinct mRNA export machineries and coordinately regulate mitotic progression. Mol. Biol. Cell **21:**2953–2965.